

RESEARCH

Open Access



# Expression of nicastrin, NICD1, and Hes1 in NCSTN knockout mice: implications for hidradenitis suppurativa, Alzheimer's, and liver cancer

Lu Yan<sup>1,2†</sup>, Yin-Sen Song<sup>2†</sup>, Jian Zhou<sup>3</sup>, Lin Zhu<sup>2</sup>, Tian-Wei Shi<sup>1,2\*</sup>, Hui-Qian Yu<sup>1\*</sup>, Zi-Qing Dong<sup>4</sup>, Wei Wang<sup>2</sup>, Ting Long<sup>2</sup>, Hao-Ying Liu<sup>2</sup>, Zhe-Ye Shi<sup>2</sup> and Jian-Guo Li<sup>1\*</sup>

## Abstract

**Background** Nicastrin, a subunit of the  $\gamma$ -secretase complex, is encoded by the NCSTN gene and regulates notch signaling, it is involved in the pathogenesis of hidradenitis suppurativa (HS), Alzheimer disease (AD), and liver cancer. However, the animal models for studying HS are relatively scarce.

**Methods** CRISPR/Cas-mediated genetic engineering was used to generate targeted knockout offspring mice (C57BL/6J). Different doses (10 mg/kg, 20 mg/kg, and 30 mg/kg) and injection methods (subcutaneous/intraperitoneal/gavage injection) of tamoxifen were used to induce the construction of NCSTN knockout mice (mice model). The expressions of nicastrin, NICD1, hes1 in skin, brain, and liver tissue in mice model and wild-type (WT) mice were measured by qRT-PCR and IHC.

**Results** The construction of mice model was successfully induced by tamoxifen, knockout efficiency was 93%, there was no difference in knockout efficiency among three doses, injection methods, genders ( $P > 0.05$ ). HS-like lesions appeared on the skin of NCSTN knockout mice after 1 month of treatment with tamoxifen, male mice had a higher number of skin lesions compared to female mice (male vs female = 76.5% vs 41.7%,  $P = 0.027$ ). Compared with WT mice, the expressions of nicastrin (skin  $P = 0.0009$ , brain  $P = 0.0194$ , liver  $P = 0.0066$ ), NICD1 (skin  $P = 0.0115$ , brain  $P = 0.0307$ , liver  $P = 0.008$ ), hes1 (skin  $P = 0.0476$ , brain  $P = 0.0143$ , liver  $P = 0.0003$ ) in mice model all decreased.

**Conclusions** The NCSTN knockout mouse might be employed as HS animal model; Reducing nicastrin may affect the expression of notch1–hes1 pathway molecules in skin, brain, and liver tissues; low dose (10 mg/kg/d) tamoxifen could be used to induce the deletion of the target gene in mice.

**Keywords** Gene knockout mice, Hidradenitis suppurativa, NCSTN, Notch, Tamoxifen

<sup>†</sup>Lu Yan and Yin-Sen Song contributed equally in this work.

\*Correspondence:

Tian-Wei Shi

stw6666@163.com

Hui-Qian Yu

hqu0202@zzu.edu.cn

Jian-Guo Li

ljg006@sina.com

Full list of author information is available at the end of the article



## Introduction

Nicastrin is a transmembrane glycoprotein that consists of a large lobe, a lobule, and a single transmembrane domain (TM), forming the  $\gamma$ -secretase complex with presenilin (PSEN), anterior pharyngeal deficient protein 1 (APH-1), and presenilin enhanced protein 2 (PEN-2) [1–3]. Nicastrin can maintain the stability of other subunits of the  $\gamma$ -secretase complex, present substrates, and act as its gatekeeper to prevent other substrates from binding to the active site [4–6].

Nicastrin is involved in the pathogenesis of hidradenitis suppurativa (HS), Alzheimer disease (AD), hepatocellular carcinoma (HCC), breast cancer, tyrosinase-dependent decolorization, and skin inflammation and is essential for the development of marginal zone and B-1 B cells, which is linked to notch signaling [7–10]. The notch pathway is involved in various stages of the growth and development of organisms, and the notch–hes1 pathway mediates the pathogenesis of many diseases [11–13]. Activating notch signaling pathway requires  $\gamma$ -secretase involvement in the final cutting, and nicastrin is genetically required for signaling from membrane-anchored activated notch [14], as an upstream factor in notch–hes1 signaling, nicastrin can be studied to find new therapeutic targets for notch–hes1 pathway related diseases.

The Cre-loxp system is a technique that controls the expression of a gene in specific tissues and at specific times, in which tamoxifen induces the Cre recombinase to recognize the loxp site and knock out a target gene [15]. Tamoxifen is an antiestrogen drug and is widely used to induce gene knockouts [16, 17]. Nevertheless, the dose of tamoxifen that are used in Cre-loxp systems vary widely, and excessive tamoxifen concentration can be toxic, > 25 mg/kg tamoxifen can damage gastric parietal cells [18]. Thus, we aimed to determine the appropriate dose of tamoxifen to reduce the incidence of side effects in mice while ensuring successful knockout of target genes. It was reported that different routes of administration may affect the efficiency of drug absorption, and the recombination efficiency of oral tamoxifen was lower than that of intraperitoneal injection [19], intraperitoneal injection of tamoxifen can inhibit the proliferation of hippocampal nerve cells in mice. Therefore, subcutaneous injection, intraperitoneal injection, and gavage injection methods were used in this study, providing preferred injection methods for future studies.

Single gene mutation of NCSTN can cause partial occurrence of HS [20], and 20 NCSTN gene mutations have been found in the HS patient cohort [21], in patients with HS, NCSTN has the highest proportion of mutations among genes in the  $\gamma$ -secretase [2], NCSTN mutant mice experience abnormal skin changes [22]. Moreover, mice in which notch1 has been genetically modified

experience hair loss and curl, and in hes1 knockout mice, hair retardation and hair stem length is reduced [23]. The quality of life of patients with HS is seriously impaired, and the impact is not limited to including the severity of HS, comorbidities, and work [24]. It is reported in up to 2% of western populations and with increasing incidence in children and adults, nearly one-third of HS cases occur in pediatric patients and nearly half of patients endorse initial symptoms in childhood [25]. Therefore, it is very necessary to study HS, we examine whether NCSTN gene knockout mice develop related skin lesions to assess their value as a mouse model of HS, and provide an animal model for the study of the pathogenesis of HS and future drug research.

Additionally, NCSTN gene also has been studied in brain and liver disease. Study [8] found that nicastrin is involved in AD, affecting the assembly and stability of GSEC-A $\beta$ n and regulating the length of A $\beta$ n. In liver disease, NCSTN promote the growth and metastasis of liver cancer cells, the expression of NCSTN is higher in liver cancer patients [9]. So we inspected the expression of NCSTN gene-related molecules in liver and brain tissues, thereby providing a novel orientation for researching the NCSTN gene and related diseases of the brain and liver.

## Materials and methods

Mice were kept in the a warm specific pathogen-free conditions animal room, given normal Co60-irradiated feed and purified water, and exposed to light for 12 h every day. All animal experiments were performed in accordance with the Guide for the Care and Use of Laboratory Animals and approved by our Institutional Review Board.

### Construction of NCSTN (floxed) mice

To create a NCSTN conditional knockout mouse model (C57BL/6J) by CRISPR/Cas-mediated genome engineering. The NCSTN gene (NCBI Reference Sequence: NM\_021607; Ensembl: ENSMUSG00000003458) is located on mouse chromosome 1, 17 exons are identified, with the ATG start codon in exon 1 and the TGA stop codon in exon 17 (Transcript: ENSMUST00000003550), exon 3–5 will be selected as conditional knockout region (cKO region), deletion of this region should result in the loss of function of the mouse NCSTN gene. To engineer the targeting vector, homologous arms and cKO region will be generated by PCR using BAC clone RP23-244J9 and RP23-476N19 from the C57BL/6 library as template. The gRNA to mouse NCSTN gene, the donor vector containing loxP sites, and Cas9 mRNA were co-injected into fertilized mouse eggs to generate targeted knockout offspring (F0). The F0 founder animals were identified by PCR followed by sequence analysis, which were bred to

wildtype mice to test germline transmission and F1 animal generation.

gRNA target sequence:

gRNA1 (matching reverse strand of gene): GATGGCCTTTTACTAGACGCTGG.

gRNA2 (matching reverse strand of gene): ACATGATCGAGGGAAACGTCAGG.

PCR Primers 1 (Annealing Temperature 60.0 °C):

5'arm forward primer: 5'-ATAGACAGACCTTTCAGACCCTT-3'.

3'loxP reverse primer: 5'-GTGGATTTCGGACCAGTCTGA-3'.

PCR Primers 2 (Annealing Temperature 60.0 °C):

5'loxP forward primer: 5'-GGACGTAAACGGCCA CAAGTTCG-3'.

3'arm reverse primer: 5'-GAAGAGCTGCATAGCACACAATG-3'.

Sequencing Primer for PCR product 1:

5'Sequence primer: 5'-CCAAGAAAGATTAAGGCCACGG-3'.

Sequencing Primer for PCR product 2:

3'Sequence primer: 5'-CGAAACCAAGGTCATCAAGCAG-3'.

**Construction of NCSTN(flox/+), CAGGCre-ERTM mice**

F0 founder animals were bred to wild-type mice to test germline transmission and F1 animal generation, inter-cross heterozygous targeted mice (F1) to generate homozygous targeted NCSTN (flox/flox) mice, breed a homozygous targeted mouse with a tissue-specific Cre delete mouse to generate mice that are heterozygous for a targeted allele and a hemizygous/heterozygous for the Cre transgene, breed heterozygous, Cre+ mice with homozygous mice. Approximately 25% of the progeny from this mating will be homozygous for the targeted allele and hemizygous/heterozygous for the Cre transgene. The pups and the tissue-specific gene deletion can be confirmed by PCR.

The reaction was 25 µL, comprising mouse genomic DNA (1.5 µL), forward primer (10 µM, 1.0 µL), reverse primer (10 µM, 1.0 µL), premixed Taq polymerase (12.5 µL), and ddH<sub>2</sub>O (9.0 µL). The cycling conditions were set as follows: initial denaturation at 94 °C for 3 min; denaturation at 94 °C for 30 s, annealing at 60 °C for 35 s, and extension at 72 °C for 35 s for a total of 35 cycles; additional extension at 72 °C for 5 min. The expected PCR product was one band at 178 bp for wild type, one band at 252 bp for homozygous, 2 bands at 252 bp and 178 bp for heterozygous and one band at 180 bp for Cre amplicon.

Primers (Annealing Temperature 60.0 °C):

Forward primer: 5'-TAGGTAAGTGTGGAATTGGGCA-3'.

Reverse primer: 5'-CCCAAGTGGATTTCATTAGAGGTCC-3'.

Cre transgene (Annealing Temperature 60.0 °C):

Forward: 5'-GCTAACCATGTTTCATGCCTTC-3'.

Reverse: 5'-AGGCAAATTTTGGTGTACGG-3'.

**Tamoxifen injection**

The study employed three distinct doses of tamoxifen (10 mg/kg/d, 20 mg/kg/d, and 30 mg/kg/d) and three different administration approaches (intraperitoneal injection, subcutaneous injection, and gavage injection) to induce the deletion of the NCSTN gene in NCSTN(flox/+), CAGGCre-ERTM mice. The body weight of mice was measured 3 times and averaged as the final value. Tamoxifen (Sigma-Aldrich, USA, T5648-1G) was dissolved in corn oil (Aladdin, C116023-500mL, China), and ultrasonic vibration was performed for 20 min to doses of 10 mg/kg, 20 mg/kg, and 30 mg/kg. The mice with the genotype NCSTN (flox/+), CAGGCre-ERTM were divided randomly into nine groups, as shown in Table 1. Injections were scheduled once per day for a total of 6 injections. Then, 21 days after injection, ear tissue of mice was harvested for genotyping by PCR. The reaction was 25 µL, comprising mouse genomic DNA (1.0 µL), forward primer (10 µM, 1.0 µL), reverse primer (10 µM, 1.0 µL), dNTPs (2.5 mM, 3 µL), 5× LongAmp Taq Reaction 5 µL, LongAmp Taq DNA Polymerase 1 µL, ddH<sub>2</sub>O 13 µL. The cycling conditions were set as follows: initial denaturation at 94 °C for 3 min; denaturation at 94 °C for 30 s, annealing at 60 °C for 30 s, and extension at 65 °C for 50 s/kb for a total of 33 cycles; additional extension at 65 °C for 10 min. The expected product was 251 bp for the KO allele. Ultimately, the number of NCSTN knockout mice in each group was enumerated.

PCR for constitutive KO allele (annealing temperature 60.0 °C):

Forward primer: (F5): 5'-TAGGTAAGTGTGGAATTGGGCA-3';

Reverse primer: (R6): 5'-ATATTCTCCTTCCACGTACTTCTGA-3'.

**Table 1** Number of mice in nine groups injected with tamoxifen

Dose	Injection method		
	subcutaneous	Intraperitoneal	Intragastric
Low (10 mg/kg)	A1 (5)	B1 (5)	C1 (5)
Medium (20 mg/kg)	A2 (5)	B2 (6)	C2 (5)
High (30 mg/kg)	A3 (6)	B3 (5)	C3 (5)

Columns A, B, and C indicate subcutaneous injection, intraperitoneal injection, and intragastric injection, respectively. 1, 2 and 3 indicate low dose (10 mg/kg), medium dose (20 mg/kg), and high dose (30 mg/kg), respectively. The numbers in brackets in the table represent the number of mice in each group

### Tissue specimens

Separately retain the skin, brain, liver tissues of NCSTN gene knockout mice or wild-type mice were placed immediately in liquid nitrogen and stored at  $-80^{\circ}\text{C}$  for qRT-PCR. The other specimens were fixed in formalin and embedded in paraffin for HE staining and IHC.

### Hematoxylin–eosin (HE) staining and immunohistochemistry (IHC)

Paraffin-embedded tissues were sectioned contiguously at a thickness of  $3\ \mu\text{m}$  on a microtome (LEICA RM2245). The slices from the skin, brain, liver tissues of NCSTN gene knockout mice and wild-type mice were placed into an automatic stainer for HE staining (Tissue-Tek Prisma<sup>®</sup> Plus Automated Slide Stainer). IHC was performed using avidin–biotin–peroxidase. Briefly, the paraffin sections were dewaxed in xylene, subjected to antigen recovery with citric acid antigen repair buffer, incubated with 3%  $\text{H}_2\text{O}_2$  to block endogenous peroxidase, and incubated for 60 min at room temperature with anti-nicastrin (abs135762; absin), anti-cleaved notch1 (Val1744) (AF5307; Affinity), and anti-hes1 (D6P2U; Cell Signaling Technology). After a wash with PBS, secondary antibody was added at room temperature for 30 min, and signals were visualized with DAB, with hematoxylin counterstaining. The slices were dehydrated with gradient ethanol and xylene and sealed with neutral gum. The expression of nicastrin, NICD1 and hes1 protein were visualized under a microscope (Leica, Germany).

### Total RNA extraction and qRT-PCR

Total RNA was extracted from skin, brain, liver tissues of NCSTN gene knockout mice and wild-type mice using the TRIzol reagent (#15596026, Invitrogen, USA) following the manufacturer's protocol. For complementary DNA (cDNA) synthesis, the reverse transcription reaction was performed using the NovoScript<sup>®</sup> Plus All-in-one 1st Strand cDNA Synthesis SuperMix (gDNA Purge) (novoprotein, China) kit. Quantitative PCR (qPCR) assays were prepared using the NovoStart<sup>®</sup> SYBR qPCR SuperMix Plus kit (novoprotein, China) and were conducted on 7500 Fast Real-Time PCR System (Applied Biosystems, USA).

For qRT-PCR, the reaction mixture consisted of  $10\ \mu\text{L}$  of  $2\times$  NovoStartRSYBR qPCR SuperMix Plus,  $0.4\ \mu\text{L}$  of ROX,  $1\ \mu\text{L}$  of cDNA, ensure that the concentrations of the forward and reverse primers are within  $0.5\ \mu\text{M}$ , and finally add RNase Free Water up to  $20\ \mu\text{L}$ . This mixture was processed in a 7500 Fast Real-Time PCR System (Applied Biosystems, Thermo Fisher Scientific, USA). The thermal cycling conditions were set as follows: pre-denaturation at  $95^{\circ}\text{C}$  for 1 min; denaturation at  $95^{\circ}\text{C}$  for

20 s; annealing at  $60^{\circ}\text{C}$  for 20 s; and extension at  $72^{\circ}\text{C}$  for 30 s for a total of 40 cycles. GAPDH served as a loading control for mRNA. The relative gene expression levels were obtained using the  $2^{-\Delta\Delta\text{Ct}}$  method. The primer sequences are listed in Table 2.

### Statistical analysis

All statistical analyses were performed using the SPSS 21.0 and GraphPad Prism 8.3 software. The qualitative data were performed with Chi-square test or the Fisher's precision probability test, and the quantitative data were expressed as mean  $\pm$  SD.  $P < 0.05$  was considered statistically significant.

## Results

### Generation of NCSTN (flox/+), CAGGCre–ERTM mice

NCSTN conditional knockout mouse model were obtained by CRISPR/Cas-mediated genome engineering, and the overview of the targeting strategy is shown in Fig. 1.

The genotyping strategy is shown in Fig. 2a. The results of F1–R1/F2–R2 PCR screening in Fig. 2a are, respectively, presented in Fig. 2b1/b2. F1 animals were identified positive by PCR screening, Fig. 2c displays the positive sequencing results of mice from the F1 generation, with the loxp site indicated by red bases. Crossing NCSTN (flox/+) mice resulted in two bands at 252 bp and 178 bp, as depicted in Fig. 3a. The CAGGCre–ERTM mice was demonstrated by a band around 180 bp shown in Fig. 3b. The NCSTN (flox/+), CAGGCre–ERTM mice were generated by crossing NCSTN (flox/+) mice with CAGGCre–ERTM mice. As shown in Fig. 4a, the same mouse showed positive bands near 252 bp and/or 178 bp (F: flox) and 180 bp (C: Cre), PCR analysis confirmed that NCSTN (flox/+), CAGGCre–ERTM mice were successfully obtained.

### Effects of tamoxifen dose, injection method, and gender on knockout

21 day post-completion of the tamoxifen injection experiment, the knockout effect of tamoxifen was detected

**Table 2** qRT-PCR primer sequences

Gene name	Primer name	Primer sequence
Mus-nicastrin	Mus-nicastrin-F	CTGGGCAACGGCTTGCTTATG
	Mus-nicastrin-R	CACAATGGGAAGCTTGGTGACG
Mus-NICD	Mus-NICD-F	CCACTGTGAAGTCCCTATGTGCC
	Mus-NICD-R	CACATTTTCTTACAGTTCTGTCC
Mus-hes1	Mus-hes1-F	GGAAATGACTGTGAAGCACCTCC
	Mus-hes1-R	GAAGCGGGTCACCTCGTTCATG

## Genotyping Strategy

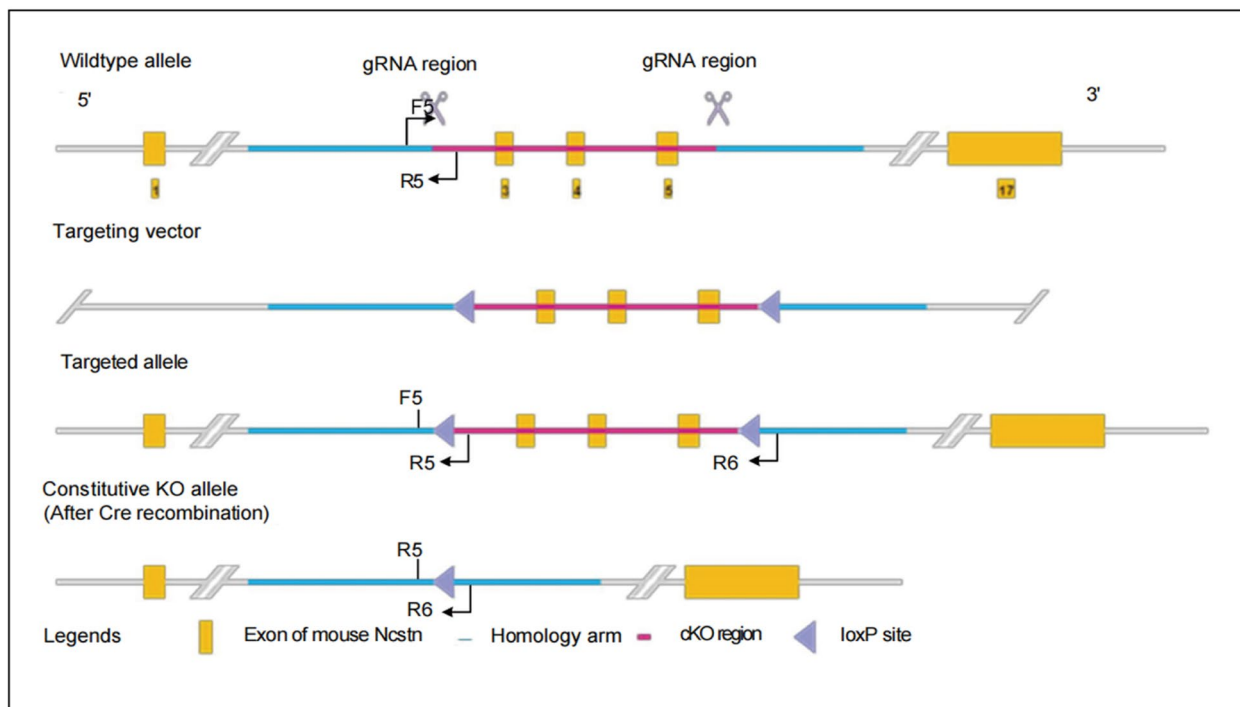


**Fig. 1** Creation of NCSTN conditional knockout mice

using PCR. All three doses and injection methods were found to be successful in inducing the target gene knockout. As shown in Fig. 4b, successful knockout of the target gene resulted in a band at approximately 180 bp.

Of the 44 mice in this experiment, NCSTN gene was successfully deleted in 41 mice, the knockout efficiency of tamoxifen was 93%. As shown in Fig. 4c1/c2, the effects of different doses or injection methods on gene knockout efficiency were found to be statistically insignificant (dose: low–medium, OR (95% CI)=1.00(0.057, 17.621),  $P=1.0$ ; low–high/medium–high, OR (95% CI)=1.077 (0.061, 19.046),  $P=0.96$ . injection: subcutaneous-peritoneal, OR (95% CI)=1.00 (0.057, 17.621),  $P=1.0$ ; subcutaneous-gavage/peritoneal-gavage, OR (95%CI)=1.077 (0.061, 19.046),  $P=0.96$ ). As shown in Fig. 4c3, the effect of gender on gene knockout efficiency was found to be statistically insignificant (OR (95% CI)=0.320 (0.027, 3.825),  $P=0.347$ ). These results suggest that the sex, dose, and application method of tamoxifen do not influence the knockout of the NCSTN.

### Pathological features of NCSTN conditional knockout mice

As shown in Fig. 5a1–4, in the construction of successful NCSTN gene knockout mice, some mice began to develop skin lesions and shed their hair after 1 month,

over time, the number of mice with these symptoms and the degree of skin lesion also increased (Fig. 5b2–4). The lesions were concentrated mainly on the posterior neck, back, groin, axilla, mouth, and nose (Fig. 5a1–4, b2–4). HE staining of skin lesions in NCSTN gene knockout mice showed epidermal thickening or reduction, hair follicle keratinization, and increased inflammatory cell infiltration (Fig. 5d1–6). We found that male mice developed symptoms more frequently, among the 17 male mice, 13 had skin lesions, and among the 24 females, 10 had skin lesions, analyzing the relationship between gender and lesions, the results indicate that gender may be involved in the occurrence of skin lesions (OR (95%CI)=4.550 (1.141, 18.151),  $P=0.027$ , Fig. 5c).

### Expression of nicastrin/NICD/hes1 in NCSTN conditional knockout mice

To investigate the expression of related molecules in several organs of NCSTN knockout mice, we detected the expression of nicastrin/NICD1/hes1 in wild-type mice and NCSTN knockout mice in skin, brain, and liver tissues using IHC and qRT-PCR. The expression of nicastrin/NICD1/hes1 in NCSTN knockout mice skin (Fig. 6a①–②, b①–②, c①–②) was consistent with our previous studies [22], compared to wild-type mice, the

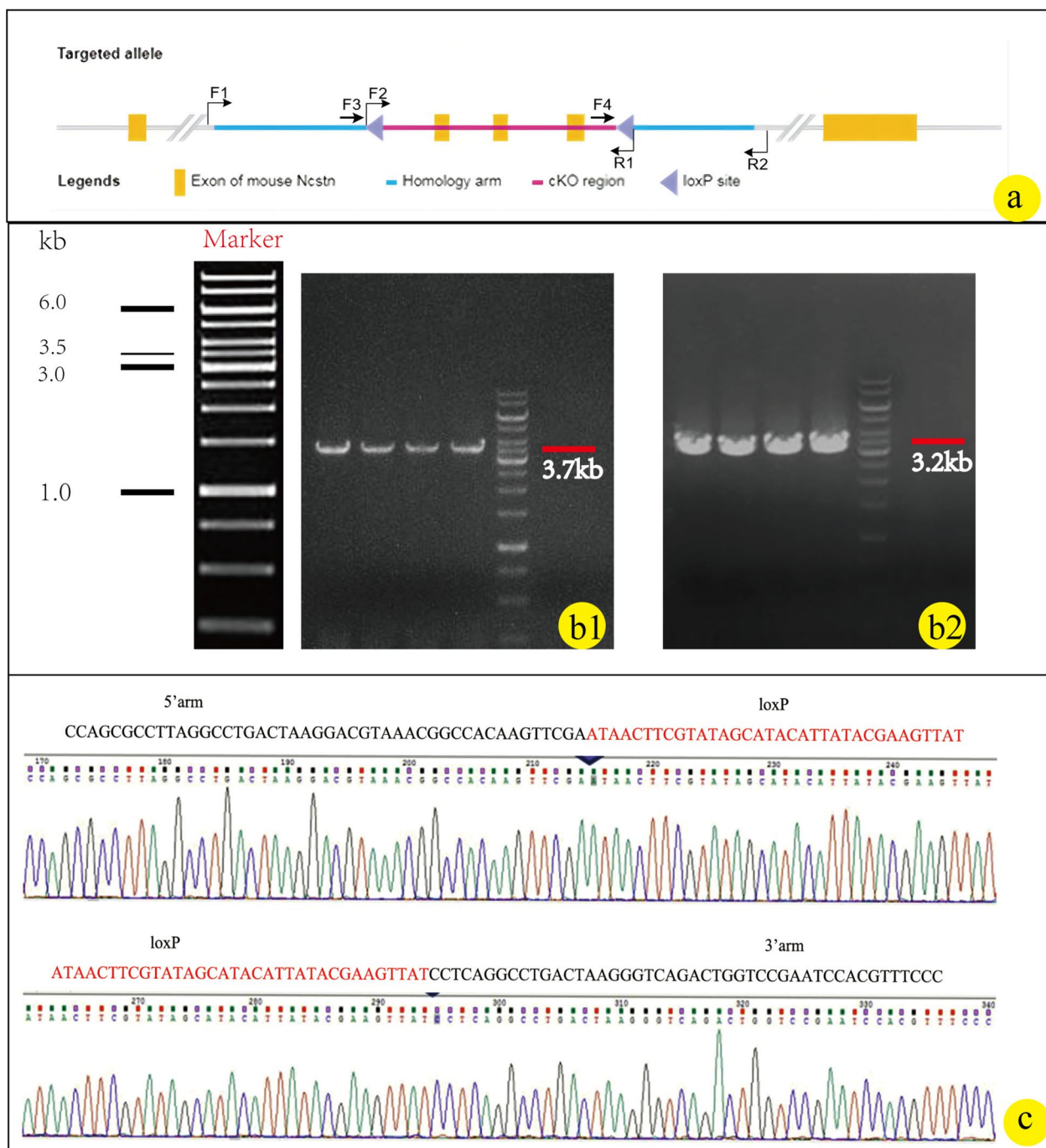


**Fig. 2** Genotyping strategy and identification results for F0 founder animals. **a** F0 founder animals' genotyping strategy. **b1/b2** **b1** Shows the target fragments from F1 to R1 (3.7 kb) and **b2** shows the target segment F2 to R2 (3.2 kb) in knockout offspring. **c** Sequencing results of loxP locus between the 5'arm and 3'arms of the target fragment in knockout offspring; the red bases in **c** are the loxP sites region

NCSTN gene knockout mice showed a decreased staining of nicastrin/NICD1/hes1 in skin tissue (Fig. 6a③–④, b③–④, c③–④). In brain, nicastrin was expressed primarily in neuronal cells and glial nuclear plasma; NICD1 was mainly expressed in glial nuclear plasma

and less in nerve cells; and hes1 was expressed in neuronal cells, and less in glial nuclear plasma (Fig. 6d①–②, e①–②, f①–②). In liver, nicastrin/NICD1/hes1 was expressed in the nucleus of hepatic sinusoidal endothelial cells (Fig. 6g①–②, h①–②, j①–②). Compared

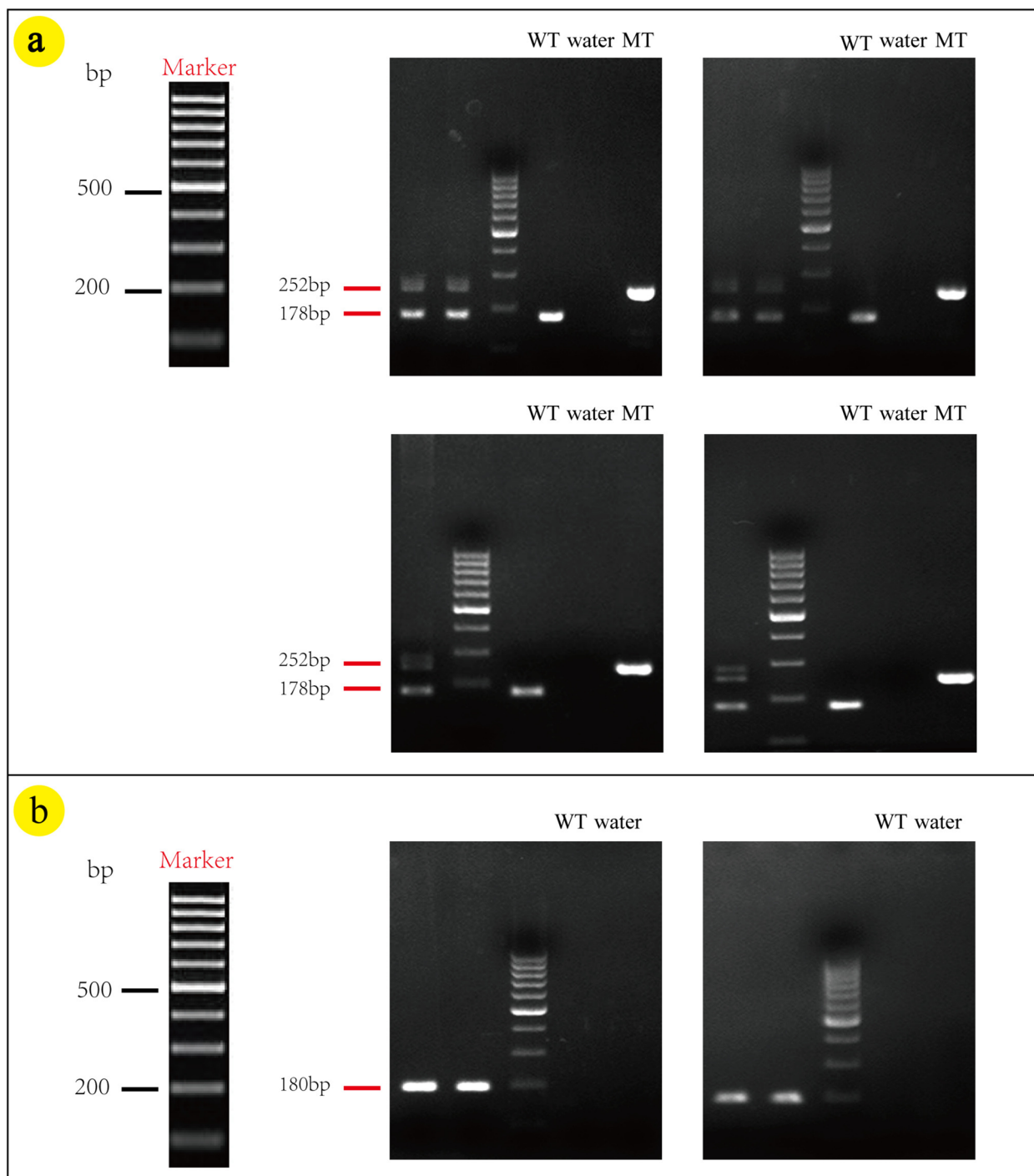


**Fig. 3** PCR target fragment size: WT (wild type): one band at 178 bp. Heterozygous (flox/+): 2 bands at 252 bp and 178 bp. Homozygous (flox/flox): 1 band at 252 bp. Cre amplicon: 180 bp. **a** PCR results: NCSTN(flox/+) mice successfully obtained that it had 2 bands at 252 bp and 178 bp. **b** PCR results: CAGGCre-ERTM mice were verified that it had 1 band at 180 bp

with wild-type mice, in the brain and liver tissues, NCSTN gene knockout mice showed lower expression of nicastrin/NICD1/hes1 (Fig. 6d③-④, e③-④, f③-④, g③-④, h③-④, j③-④). We also assessed the

expression levels of nicastrin/NICD1/hes1 mRNA, the results showed that compared with WT mice, the expressions of nicastrin (skin  $P=0.0009$ , brain  $P=0.0194$ , liver  $P=0.0066$ ), NICD1 (skin  $P=0.0115$ , brain  $P=0.0307$ ,

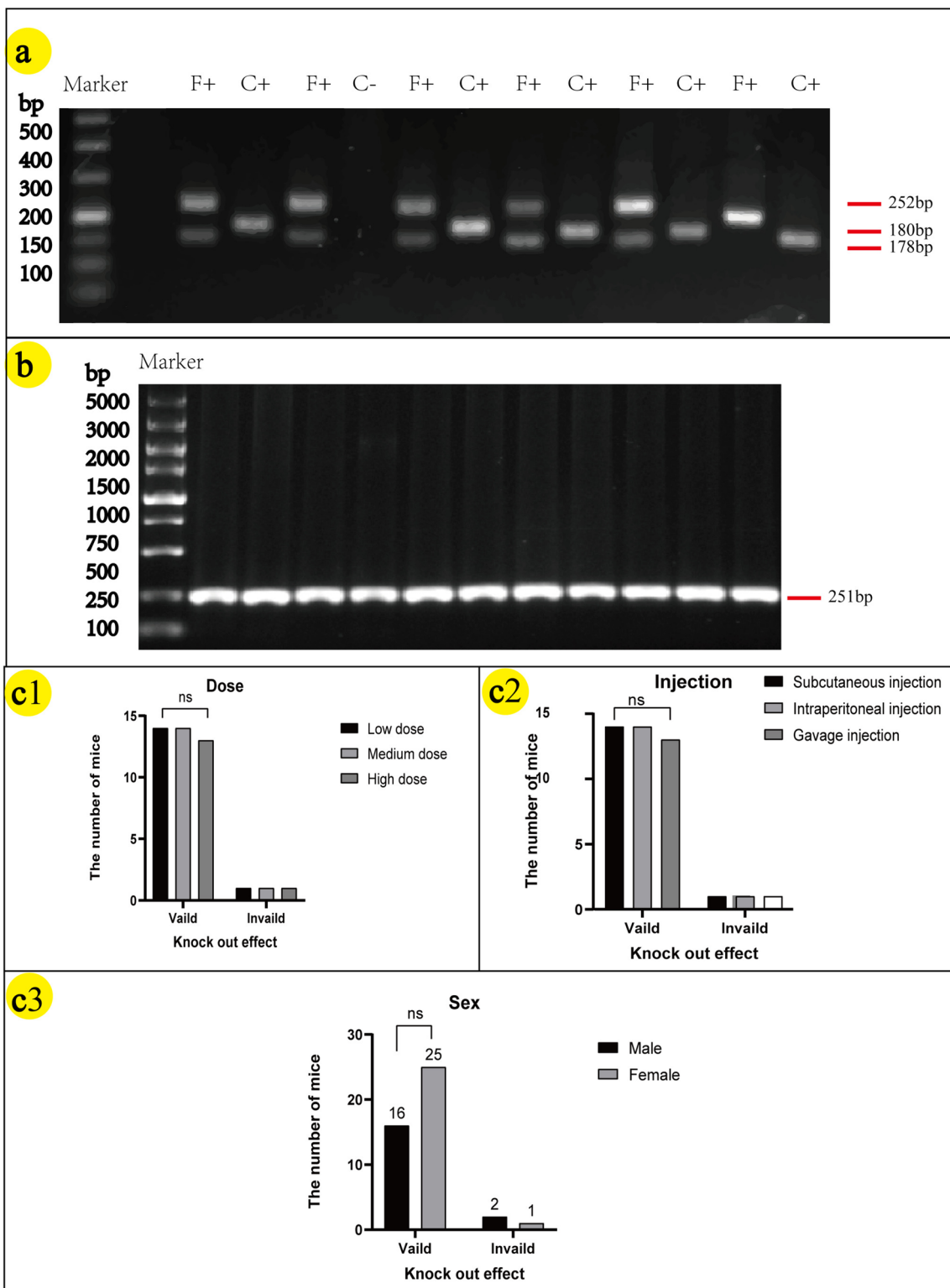


**Fig. 4** **a** PCR results in NCSTN(flox/ +),CAGGCre–ERTM mice; F + express F-positive and C + express C-positive bands (F: flox—252 bp + 178 bp; C: cre—180 bp). **b** PCR results of successful deletion of NCSTN in mice injected with tamoxifen. In figure **b**, all mice showed 1 band at around 251 bp. **c1/c2/c3** **c1**, **c2** and **c3** show the relationship between tamoxifen dose, application method, sex, and knock-out efficiency, respectively; statistical analysis using chi-square test,  $P > 0.05$  express ns. Low dose: 10 mg/kg/day; medium dose: 20 mg/kg/day; high dose: 30 mg/kg/day



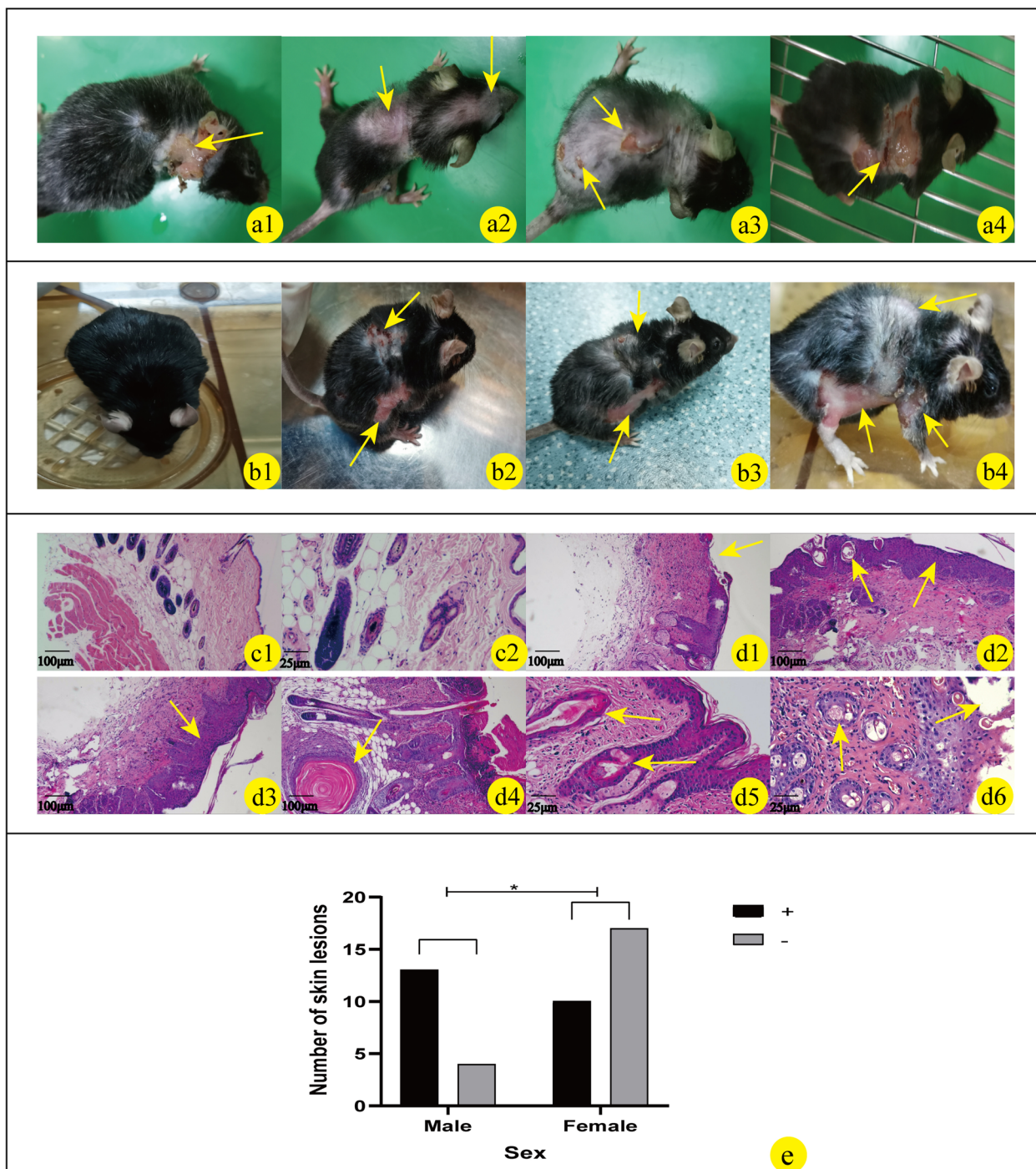


**Fig. 5** Phenotypic changes in skin of NCSTN gene knockout mice; the skin lesions include shedding hair, recurrent inflammatory papules, plaques, pustules, cysts, ulcer, and scars. The above skin lesions are mainly concentrated in the posterior neck (a1), back (a2, a3, a4), groin (b2–b4), axilla (b4), and mouth and nose (a2) (as shown by yellow arrows). b1–b4 show the changes in skin phenotypes over time in the same NCSTN gene knockout mice without tamoxifen (b1) and after tamoxifen injection (b2–b4). The observation time of the skin phenotype was recorded after induction of NCSTN gene knockout mice with tamoxifen (b2 > 6 weeks, b3 > 10 weeks, b4 > 6 months) (as shown by the yellow arrow). c1–d6: Microscopic features of skin in wild type and NCSTN gene knockout mice; c1 and c2 are pathological manifestations of skin in wild-type mice (c1 × 100; c2 × 400). Compared with the microstructure of skin tissue in wild-type mice, NCSTN gene knockout mice show epidermal thickening (d2 × 100, d3 × 100), increased inflammatory cells (d2 × 100, d3 × 100), keratosis of hair follicles (d2 × 100, d4 × 100, d5 × 400), fewer hair follicles (d1 × 100, d2 × 100), and full-layer loss of epidermis in severe cases (d1 × 100, d6 × 400). These skin manifestations are shown by yellow arrows. e Relationship between sex (male VS female) and skin lesion phenotype in NCSTN gene knockout mice by Fisher’s exact test,  $P < 0.05$ . This result shows that the sex of mice correlates with skin lesion (+: skin lesions; -: normal)

liver  $P=0.008$ ), *hes1* (skin  $P=0.0476$ , brain  $P=0.0143$ , liver  $P=0.0003$ ) in mice model all decreased ( $P<0.05$ , Fig. 7a–c), and the result is statistically significant.

## Discussion

Nicastrin is a subunit of the  $\gamma$ -secretase that cleaves integral membrane proteins, including notch receptors and beta-amyloid precursor protein, and may be a stabilizing cofactor that is required for  $\gamma$ -secretase assembly [1]. The  $\gamma$ -secretase is involved in the third step of notch cleavage, converting inactive notch into active NICD, which then enters the nucleus and binds downstream signaling molecules. Notch protein is widely expressed in a variety of species and primarily transmits signals from cell to cell, ultimately determining cell fate and influencing organ formation and morphogenesis. Studies [11] shown that nicastrin is closely related to the notch pathway.

In this study, NCSTN (flox/+), CAGGCre–ERTM mice were induced by tamoxifen, tamoxifen is an estrogen receptor ligand that is widely used in inducible gene knockout models. However, tamoxifen is toxic over a certain dose, and its concentration correlates positively with drug toxicity [26]. In the construction of knockout mice, the dose of tamoxifen affects the growth of normal bone tissue, and doses over 25 mg/kg can damage gastric cells [18, 27]. Thus, the appropriate dose of tamoxifen can reduce its toxic and side effects on mice and prevent abnormal lesions from forming in NCSTN conditional knockout mice. We used 3 low dosages of tamoxifen (10 mg/kg/day, 20 mg/kg/day, and 30 mg/kg/day) for 6 days in the induction phase, all of which successfully deleted the target gene. On the other hand, the knockout efficiency in different route of administration was consistent in this experiment. Induction by tamoxifen has been reported [28] to be more readily absorbed by gavage, thus, gavage injection and low dose administration should be prioritized to increase drug absorption and reduce the side effects of tamoxifen.

As a notch classical pathway, notch–*hes1* signaling [29–31] has been studied widely in diseases that involve the blood, digestive, respiratory, reproductive, skeletal,

and nervous systems, and the activity of the  $\gamma$ -secretase complex and notch signaling is affected when nicastrin is inhibited [32]. The study showed that the expression of NICD1 and *hes1* in the skin tissue of HS patients was decreased compared with that of normal skin [33], one cell experiments [34] showed that after treatment of hair follicle stem cells with DAPT, a  $\gamma$ -secretase inhibitor, NICD and *hes1* were downregulated. In the present experiment, we found that the protein and mRNA expression of nicastrin, NICD1 and *hes1* decreased in the skin, brain, and liver of the NCSTN gene knockout mice, this results supports that knockout NCSTN gene can down-regulate notch1 and *hes1* expression, and the NCSTN gene knockout mice model may study diseases that involve the nicastrin–notch1–*hes1* pathway. Meanwhile, there are few study report the role of *hes1* in HS, NCSTN conditional knockout mice may be used to study the role of notch1–*hes1* in HS in the future.

Approximately 4 weeks after injection, some NCSTN gene knockout mice showed pathological changes in the skin, such as recurrent inflammatory papules, plaques, pustules, cysts, ulcer, and scars on the posterior neck, back, groin, axilla, mouth, and nose, with time increasing, more mice developed skin lesions and shed their hair, and the skin was thick and hard around the scar-like lesions. These abnormal skin changes were similar to those that have been reported in patients with HS [35]. By HE staining, the skin lesions showed thickening of the epidermis, fewer hair follicles, and keratinization of hair follicles, consistent with the pathological results of clinical patients with HS [36]. One case report [36] showed that in HS patients, notch1 and NCSTN mRNA expression decreased in the lesion skin, this result suggested that the low expression of nicastrin may be related to the occurrence of HS. Combined with the similar lesions in experiment mouse, this result support the NCSTN conditional knockout mice may be as animal model to study the HS. Furthermore, one report suggests that a patient taking a GSC inhibitor exhibited skin changes similar to those of HS, and the patient explicitly affirmed that the GSC inhibitor was associated with the skin lesion [37].

(See figure on next page.)

**Fig. 6** Immunohistochemistry of skin, brain, and liver specimens of wild-type mice (a1–j1  $\times 100$ ; a2–j2  $\times 400$ ) and NCSTN gene knockout mice (a3–j3  $\times 100$ ; a4–j4  $\times 400$ ). Staining for nicastrin (WT-a1/a2 and NCSTN gene knockout mice-a3/a4), NICD1 (WT-b1/b2 and NCSTN gene knockout mice-b3/b4), and *hes1* (WT-c1/c2 and NCSTN gene knockout mice-c3/c4) in skin tissues mainly in epidermis and hair follicles; in brain tissues, staining for nicastrin (WT-d1/d2 and NCSTN gene knockout mice-d3/d4) mainly in neuronal cells and glial nuclear plasma. NICD1 (WT-e1/e2 and NCSTN gene knockout mice-e3/e4) mainly expressed in glial nuclear plasma, with a small amount in nerve cells, and *hes1* (WT-f1/f2 and NCSTN gene knockout mice-f3/f4) expressed in neuronal cells, with a small amount in glial nuclear plasma. In liver tissues, staining for nicastrin (WT-g1/g2 and NCSTN gene knockout mice-g3/g4), NICD1 (WT-h1/h2 and NCSTN gene knockout mice-h3/h4), and *hes1* (WT-j1/j2 and NCSTN gene knockout mice-j3/j4) mainly in the nucleus of hepatic sinusoidal endothelial cells. Compared with wild-type mice (a1–j1, a2–j2), the expression of these proteins in skin, brain and liver tissue was lower in NCSTN gene knockout mice (a3–j3, a4–j4)

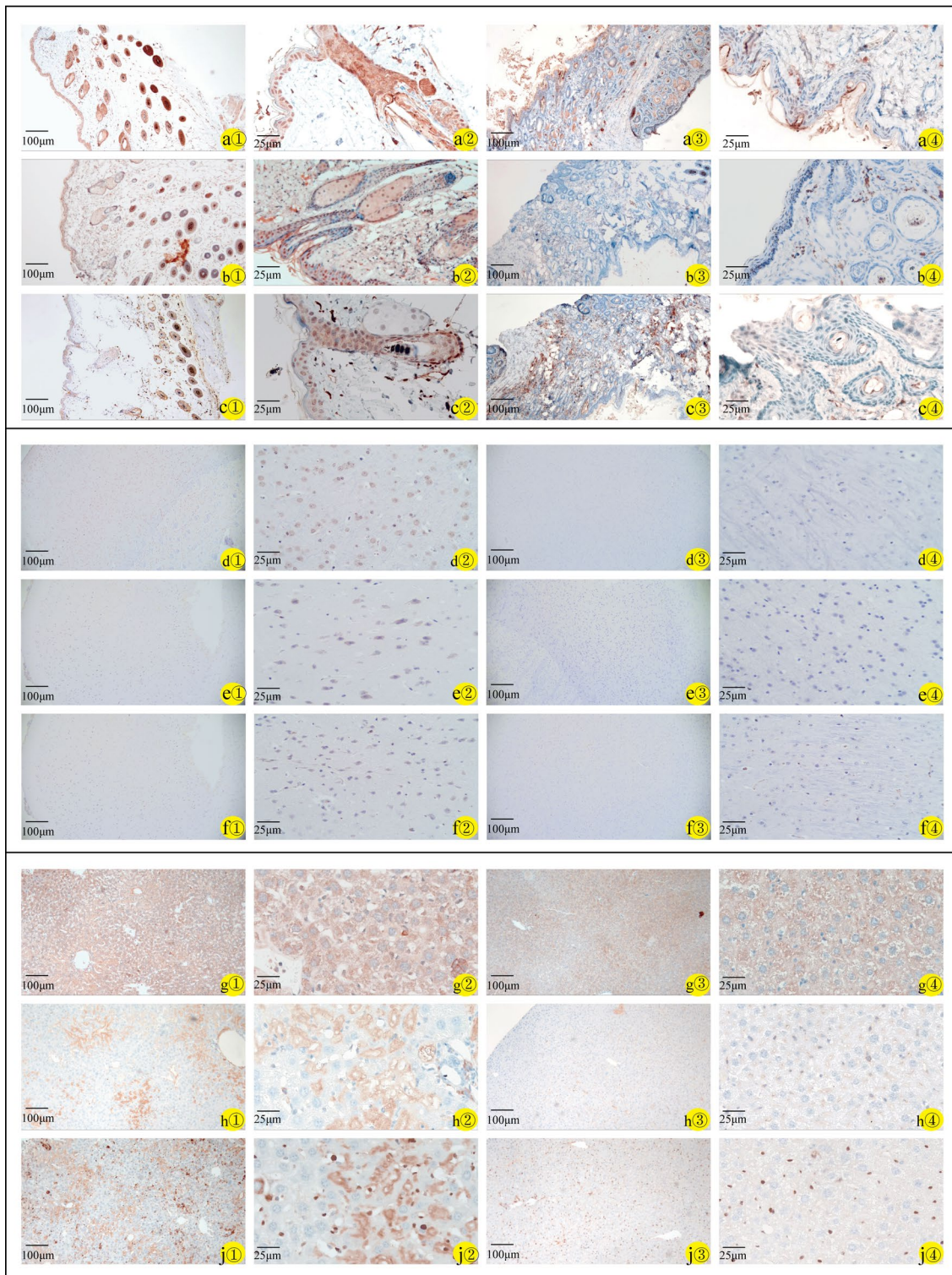


**Fig. 6** (See legend on previous page.)

In our study, NCSTN gene-knockout mouse models presented skin lesions similar to those of HS, we hypothesize that the downregulation of NCSTN might be related to

the skin lesions, perhaps increasing the expression of NCSTN in HS patients could be beneficial, and the next step might be to attempt to increase NCSTN expression

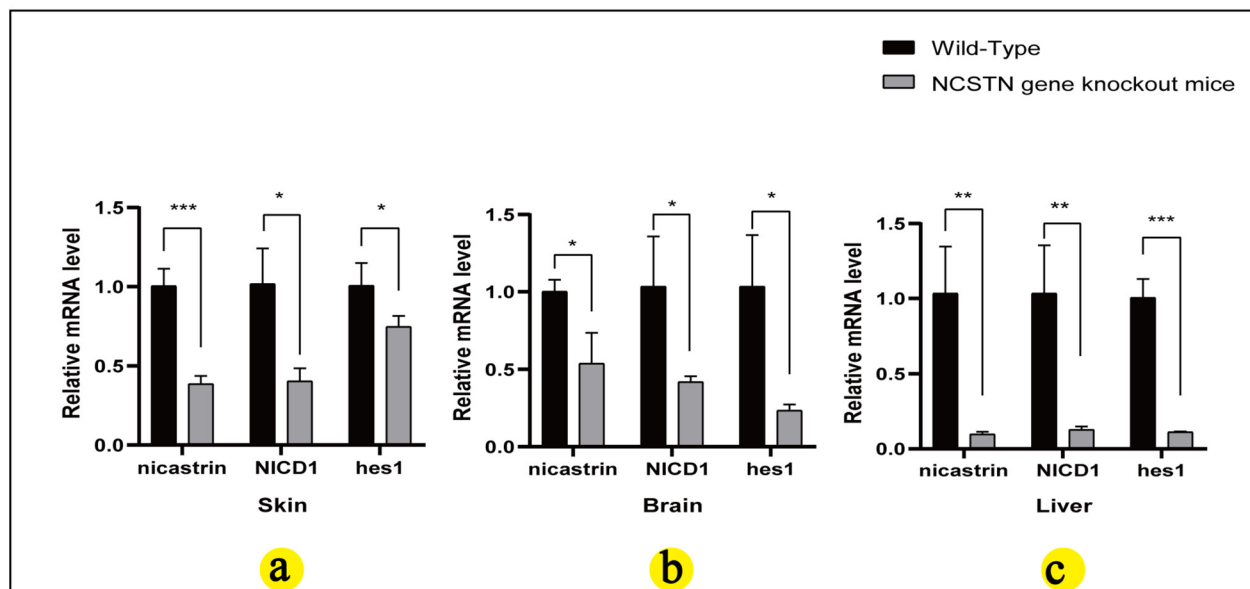


**Fig. 7** Nicastrin, NICD1, and hes1 mRNA in skin (a), brain (b), and liver (c) of wild-type and NCSTN gene knockout mice. Relative mRNA expression level of nicastrin, NICD1, and hes1 in wild-type mice ( $n=3$ ) and NCSTN gene knockout mice ( $n=3$ ), by qRT-PCR, using the  $2^{-\Delta\Delta CT}$  method and student's  $t$  test. Compared wild-type mice, mRNA levels of nicastrin, NICD1, and hes1 in skin (a), brain (b), and liver (c) of NCSTN gene knockout mice were all decrease (\* $P < 0.05$ ; \*\* $P < 0.01$ ; \*\*\* $P < 0.001$ )

and observe changes in skin lesions to offer a promising direction for HS diseases.

In this mouse model, which developed skin lesions, we found that males developed symptoms earlier and more severely than females, and in our statistical analysis, sex correlated with skin lesions. According to research reports, In Western countries, women are more likely to develop hidradenitis suppurativa than men, but in Eastern countries, the ratio is reversed [38]. Males predominance in Asian populations, and male is associated with greater involvement in the buttocks, perianal and posterior neck [39]. In this study, we also observed a higher distribution of skin lesions in the neck in male mice, but the number of experimental mice is small and needs to be further expanded. A meta-analysis included 10 studies with a total of 30,125 patients with HS, the male-to-female ratio of East and Southeast Asian HS patients was 0.66, Subgroup analysis by country found the pooled proportion of male HS patients to be 0.72 in Japan, 0.67 in Malaysia, and 0.66 in South Korea [40]. HS predominantly affects males in Japan [35]. In lineages of familial HS, there are more male patients [35, 41, 42], and Nishimori et al. [42] have reported that women have fewer symptoms than men. Our findings are consistent with these studies and support that gender is involved in HS.

Currently, there have been a few studies reporting that NCSTN may be involved in the development of brain and liver diseases. Research shows Nicastrin

can act as a gatekeeper in AD, preventing inappropriate protein cleavage, having a unique advantage of its large size [43], inhibiting the Musashi1/Notch1/Hes1 signal may play a crucial role in learning and memory deficits, neural plasticity function disorders, and astrocyte hyperplasia[44]. Notch1/hes1 signaling was found to play a key role in the pathogenesis of liver injury [45], and the abnormally activated notch1–hes1 signaling pathway may be related to the formation of biliary cysts in polycystic liver [29]. Maintaining hes1 at a reasonable level plays a related role in liver fibrosis [46]. Some studies [9] also found that NCSTN can promote the growth and metastasis of hepatocellular carcinoma cells, and a notch inhibitor that is based on nicastrin can reduce liver fibrosis [47]. In our research result, the expression of nicastrin, NICD1, and hes1 in the brain and liver tissue of NCSTN gene knockout mice were downregulation. Consequently, the results might be utilized as an interesting direction to investigate the brain and liver diseases associated with notch1–hes1 signaling pathway.

Due to the small number of experimental animals, it is necessary to expand the cohort to verify the occurrence of the phenomena above and study the mechanisms of these results. In this study, only HS-like lesions were observed through pathology, and relevant inflammatory factors were not further studied, the relevant mechanisms of this aspect will be further explored in the later stage.

## Conclusion

Ultimately, we generated NCSTN gene knockout mice through genetic engineering and administer tamoxifen injection, and found that low dosages (10 mg/kg) and gavage injections maybe applied preferentially to knock out the target gene. In NCSTN gene knockout mice, we thought that the lesion bears resemblance to HS, and they have the potential to be employed as an HS animal model for related research which including pathogenic mechanism and therapeutic drugs. Additionally, the downregulation of nicastrin expression in skin, brain and liver tissues can exert an influence on the expression of NICD1 and *hes1*, and future research may delve into the manner in which the NCSTN–notch signaling pathway affects skin, brain and liver-related disorders, providing a novel research orientation for related diseases.

## Acknowledgements

Not applicable.

## Author contributions

YL wrote the main manuscript text; SY, STW, YHQ, LJG designed of the work; ZJ, ZL, DZQ, WW, LT, LHY, SZY acquired and analysis data; YL, ZL interpreted the data; YL, STW had drafted the work and substantively revised it. All authors reviewed the manuscript.

## Funding

This study was supported by National Natural Science Foundation of China (No. 81773344) and the Medical Scientific and Technological Project of Henan Province (No. LHGJ20200685).

## Availability of data and materials

No datasets were generated or analysed during the current study.

## Declarations

### Ethics approval and consent to participate

All animal experiments were performed in accordance with the Guide for the Care and Use of Laboratory Animals and approved by the Fifth Clinical Medical College of Henan University of Chinese Medicine Institutional Review Board (ID: KY2021-004-01-D).

### Consent for publication

Not applicable.

### Competing interests

The authors declare no competing interests.

### Author details

<sup>1</sup>Henan Provincial People's Hospital, Zhengzhou University People's Hospital, Henan University People's Hospital, No. 7 Weiwu, Zhengzhou 450003, Henan, China. <sup>2</sup>The Fifth Clinical Medical College of Henan University of Chinese Medicine (Zhengzhou People's Hospital), The Affiliated Zhengzhou People's Hospital of Xinxiang Medical University, The Affiliated Zhengzhou People's Hospital of Southern Medical University, No. 33 Huanghe Road, Zhengzhou, China. <sup>3</sup>Henan Cancer Hospital (Affiliated Cancer Hospital of Zhengzhou University), 127 Dongming Rd, Zhengzhou, China. <sup>4</sup>Nanfeng Hospital, Southern Medical University, No. 1838 North Guangzhou Avenue, Baiyun District, Guangzhou, China.

Received: 19 October 2024 Accepted: 15 December 2024

Published online: 24 December 2024

## References

1. Yu G, Nishimura M, Arawaka S, Levitan D, Zhang L, Tandon A, et al. Nicastrin modulates presenilin-mediated notch/glp-1 signal transduction and betaAPP processing. *Nature*. 2000;407(6800):48–54.
2. Wang Z, Yan Y, Wang B.  $\gamma$ -Secretase genetics of hidradenitis suppurativa: a systematic literature review. *Dermatology*. 2021;237(5):698–704.
3. Escamilla-Ayala A, Wouters R, Sannerud R, Annaert W. Contribution of the Presenilins in the cell biology, structure and function of  $\gamma$ -secretase. *Semin Cell Dev Biol*. 2020;105:12–26.
4. Zhang YW, Luo WJ, Wang H, Lin P, Vetrivel KS, Liao F, et al. Nicastrin is critical for stability and trafficking but not association of other presenilin/ $\gamma$ -secretase components. *J Biol Chem*. 2005;280(17):17020–6.
5. Bolduc DM, Montagna DR, Gu Y, Selkoe DJ, Wolfe MS. Nicastrin functions to sterically hinder  $\gamma$ -secretase-substrate interactions driven by substrate transmembrane domain. *Proc Natl Acad Sci USA*. 2016;113(5):E509–18.
6. Shah S, Lee SF, Tabuchi K, Hao YH, Yu C, LaPlant Q, et al. Nicastrin functions as a  $\gamma$ -secretase-substrate receptor. *Cell*. 2005;122(3):435–47.
7. Wang B, Yang W, Wen W, Sun J, Su B, Liu B, et al. Gamma-secretase gene mutations in familial acne inversa. *Science*. 2010;330(6007):1065.
8. Petit D, Hitzenberger M, Lismont S, Zoltowska KM, Ryan NS, Mercken M, et al. Extracellular interface between APP and Nicastrin regulates A $\beta$  length and response to  $\gamma$ -secretase modulators. *EMBO J*. 2019;38(12):e101494.
9. Wang X, Wang X, Xu Y, Yan M, Li W, Chen J, et al. Effect of nicastrin on hepatocellular carcinoma proliferation and apoptosis through PI3K/AKT signalling pathway modulation. *Cancer Cell Int*. 2020;20:91.
10. Lombardo Y, Filipović A, Molyneux G, Periyasamy M, Giamas G, Hu Y, et al. Nicastrin regulates breast cancer stem cell properties and tumor growth in vitro and in vivo. *Proc Natl Acad Sci USA*. 2012;109(41):16558–63.
11. Kopan R, Goate A. Aph-2/Nicastrin: an essential component of gamma-secretase and regulator of Notch signaling and Presenilin localization. *Neuron*. 2002;33(3):321–4.
12. Rani A, Greenlaw R, Smith RA, Galustian C. HES1 in immunity and cancer. *Cytokine Growth Factor Rev*. 2016;30:113–7.
13. Kuriyama K, Kodama Y, Shiokawa M, Nishikawa Y, Marui S, Kuwada T, et al. Essential role of Notch/Hes1 signaling in postnatal pancreatic exocrine development. *J Gastroenterol*. 2021;56(7):673–87.
14. Hu Y, Ye Y, Fortini ME. Nicastrin is required for gamma-secretase cleavage of the Drosophila Notch receptor. *Dev Cell*. 2002;2(1):69–78.
15. Kim H, Kim M, Im SK, Fang S. Mouse Cre-LoxP system: general principles to determine tissue-specific roles of target genes. *Lab Anim Res*. 2018;34(4):147–59.
16. Zhao L, Wang B, Gomez NA, de Avila JM, Zhu MJ, Du M. Even a low dose of tamoxifen profoundly induces adipose tissue browning in female mice. *Int J Obes (Lond)*. 2020;44(1):226–34.
17. Donocoff RS, Teteloshvili N, Chung H, Shoulson R, Creusot RJ. Optimization of tamoxifen-induced Cre activity and its effect on immune cell populations. *Sci Rep*. 2020;10(1):15244.
18. Keeley TM, Horita N, Samuelson LC. Tamoxifen-induced gastric injury: effects of dose and method of administration. *Cell Mol Gastroenterol Hepatol*. 2019;8(3):365–7.
19. Smith BM, Saulsbery AI, Sarchet P, Devasthali N, Einstein D, Kirby ED. Oral and injected tamoxifen alter adult hippocampal neurogenesis in female and male mice. *eNeuro*. 2022;9(2).
20. Mintoff D, Pace NP, Borg I. NCSTN in-frame deletion in maltese patients with hidradenitis suppurativa. *JAMA Dermatol*. 2023;159(9):939–44.
21. Liu M, Davis JW, Idler KB, Mostafa NM, Okun MM, Waring JF. Genetic analysis of NCSTN for potential association with hidradenitis suppurativa in familial and nonfamilial patients. *Br J Dermatol*. 2016;175(2):414–6.
22. Shi TW, Cao W, Zhao QZ, Yu HX, Zhang SS, Hao YB. Effects of NCSTN mutation on hair follicle components in mice. *Dermatology*. 2023;239(1):60–71.
23. Suen WJ, Li ST, Yang LT. Hes1 regulates anagen initiation and hair follicle regeneration through modulation of hedgehog signaling. *Stem Cells*. 2020;38(2):301–14.
24. Chernyshov PV, Finlay AY, Tomas-Aragones L, Poot F, Sampogna F, Marron SE, et al. Quality of life in hidradenitis suppurativa: an update. *Int J Environ Res Public Health*. 2021;18(11):6131.
25. Cotton CH, Chen SX, Hussain SH, Lara-Corrales I, Zaenglein AL. Hidradenitis suppurativa in pediatric patients. *Pediatrics*. 2023;151(5):e2022061049.

26. Jardí F, Laurent MR, Dubois V, Khalil R, Deboel L, Schollaert D, et al. A shortened tamoxifen induction scheme to induce CreER recombinase without side effects on the male mouse skeleton. *Mol Cell Endocrinol*. 2017;452:57–63.
27. Zhong ZA, Sun W, Chen H, Zhang H, Lay YE, Lane NE, et al. Optimizing tamoxifen-inducible Cre/loxP system to reduce tamoxifen effect on bone turnover in long bones of young mice. *Bone*. 2015;81:614–9.
28. Andersson KB, Winer LH, Mørk HK, Molkenin JD, Jaisser F. Tamoxifen administration routes and dosage for inducible Cre-mediated gene disruption in mouse hearts. *Transgenic Res*. 2010;19(4):715–25.
29. Takahashi K, Sato Y, Yamamura M, Nakada S, Tamano Y, Sasaki M, et al. Notch-Hes1 signaling activation in Caroli disease and polycystic liver disease. *Pathol Int*. 2021;71(8):521–9.
30. Kannan S, Fang W, Song G, Mullighan CG, Hammitt R, McMurray J, et al. Notch/HES1-mediated PARP1 activation: a cell type-specific mechanism for tumor suppression. *Blood*. 2011;117(10):2891–900.
31. Zhang D, Zhang D, Yang X, Li Q, Zhang R, Xiong Y. The role of selenium-mediated Notch/Hes1 signaling pathway in kashin-beck disease patients and cartilage injury models. *Biol Trace Elem Res*. 2023;201(6):2765–74.
32. Hayashi I, Takatori S, Urano Y, Miyake Y, Takagi J, Sakata-Yanagimoto M, et al. Neutralization of the  $\gamma$ -secretase activity by monoclonal antibody against extracellular domain of nicastrin. *Oncogene*. 2012;31(6):787–98.
33. Stabell SH, Renzi A, Nilsen HR, Antonsen OH, Fosse JH, Haraldsen G, et al. Detection of native, activated Notch receptors in normal human apocrine-bearing skin and in hidradenitis suppurativa. *Exp Dermatol*. 2024;33(1): e14977.
34. Jiang J, Miao Y, Xiao S, Zhang Z, Hu Z. DAPT in the control of human hair follicle stem cell proliferation and differentiation. *Postepy Dermatol Alergol*. 2014;31(4):201–6.
35. Nomura Y, Nomura T, Suzuki S, Takeda M, Mizuno O, Ohguchi Y, et al. A novel NCSTN mutation alone may be insufficient for the development of familial hidradenitis suppurativa. *J Dermatol Sci*. 2014;74(2):180–2.
36. Cortez Cardoso Penha R, Cortez de Almeida RF, Câmara Mariz J, Brewer Lisboa L, do Nascimento Barbosa L, Souto da Silva R. The deregulation of NOTCH pathway, inflammatory cytokines, and keratinization genes in two Dowling-Degos disease patients with hidradenitis suppurativa. *Am J Med Genet A*. 2020;182(11):2662–5.
37. Ríos-Viñuela E, Hoyas-Rodríguez I, Cullen-Aravena D, Martín-Broto J, Hindi N, Eraña I, et al. Hidradenitis suppurativa secondary to treatment with a gamma secretase inhibitor. *J Eur Acad Dermatol Venereol*. 2024;38(3):e219–21.
38. Chu CB, Yang CC, Tsai SJ. Hidradenitis suppurativa: disease pathophysiology and sex hormones. *Chin J Physiol*. 2021;64(6):257–65.
39. Rosi E, Fastame MT, Silvi G, Guerra P, Nunziati G, Di Cesare A, et al. Hidradenitis suppurativa: the influence of gender, the importance of trigger factors and the implications for patient habits. *Biomedicines*. 2022;10(11):2973.
40. Gotesman RD, Choi C, Alavi A. Hidradenitis suppurativa in East and Southeast Asian populations: a systematic review and meta-analysis. *Int J Dermatol*. 2021;60(11):e433–9.
41. Zhang C, Wang L, Chen L, Ren W, Mei A, Chen X, et al. Two novel mutations of the NCSTN gene in Chinese familial acne inverse. *J Eur Acad Dermatol Venereol*. 2013;27(12):1571–4.
42. Nishimori N, Hayama K, Kimura K, Fujita H, Fujiwara K, Terui T. A novel NCSTN gene mutation in a Japanese family with hidradenitis suppurativa. *Acta Derm Venereol*. 2020;100(17):adv00283.
43. Urban S. Nicastrin guards Alzheimer's gate. *Proc Natl Acad Sci USA*. 2016;113(5):1112–4.
44. Zhang S, Wang P, Ren L, Hu C, Bi J. Protective effect of melatonin on soluble  $A\beta$ 1–42-induced memory impairment, astrogliosis, and synaptic dysfunction via the Musashi1/Notch1/Hes1 signaling pathway in the rat hippocampus. *Alzheimers Res Ther*. 2016;8(1):40.
45. Radwan SM, Abdel-Latif GA, Abbas SS, Elmongy NF, Wasfey EF. The beneficial effects of L-carnitine and infliximab in methotrexate-induced hepatotoxicity: emphasis on Notch1/Hes-1 signaling. *Arch Pharm (Weinheim)*. 2023;356(11): e2300312.
46. Li X, Li Y, Zhang W, Jiang F, Lin L, Wang Y, et al. The IGF2BP3/Notch/Jag1 pathway: a key regulator of hepatic stellate cell ferroptosis in liver fibrosis. *Clin Transl Med*. 2024;14(8): e1793.
47. Zhu C, Kim K, Wang X, Bartolome A, Salomao M, Dongiovanni P, et al. Hepatocyte Notch activation induces liver fibrosis in nonalcoholic steatohepatitis. *Sci Transl Med*. 2018;10(468):eaat0344.

## Publisher's Note

Springer Nature remains neutral with regard to jurisdictional claims in published maps and institutional affiliations.